Collective ow and two-pion correlations from a relativistic hydrodynam ic model with early chemical freeze out

Tetsufum i Hirano<sup>1</sup>, and Keiichi Tsuda<sup>2</sup>

<sup>1</sup>Physics Department, University of Tokyo, Tokyo 113-0033, Japan

<sup>2</sup>D epartm ent of Physics, W aseda University, Tokyo 169-8555, Japan

(Dated: February 9, 2020)

# Abstract

We investigate thee ect of early chem ical freeze-out on radial ow, elliptic ow and HBT radii by using a fully three dimensional hydrodynamic model. When we take account of the early chemical freeze-out, the space-time evolution of temperature in the hadron phase is considerably dierent from the conventional model in which chemical equilibrium is always assumed. As a result, we not that radial and elliptic ows are suppressed and that the lifetime and the spatial size of the uid are reduced. We analyze the pt spectrum, the dierential elliptic ow, and the HBT radii at the RHIC energy by using hydrodynamics with chemically non-equilibrium equation of state.

PACS num bers:  $25.75 \, \text{Ld}$ ,  $24.10 \, \text{Nz}$ 

E lectronic address: hirano@ nt.phys.s.u-tokyo.ac.p

#### I. INTRODUCTION

One of the main topics in the physics of relativistic heavy-ion collisions is to give a detailed description of space-time evolution for the hot and dense nuclear matter by using a dynam ical model such as kinetic transport models [1] or hydrodynamics [2]. Recent experimental data at the RHIC energy suggest that we may see the signicant elect of jet quenching in transverse m om entum distribution for neutralpions [3] or azim uthal asym m etry for charged hadrons [4]. So hydrodynam ic simulations of expanding hot and/or dense matter are indispensable in quantitatively estimating the e ect of the medium on the jet quenching [5]. One of the authors (TH.) has already built a fully three dimensional hydrodynamic model which describes not only central but also non-central collisions [6]. In contrary to other hydrodynam ic models, e.g., (2+1) dimensional models with the Bjorken's scaling solution [7, 8, 9] or (3+1) dimensional models with cylindrical symmetry along the collision axis [10, 11, 12, 13], full (3+1) dimensional hydrodynam ic models [14, 15, 16, 17, 18, 19] enables us to obtain the rapidity dependence of particle distribution, elliptic ow, and HBT radii. in non-central collisions. To give a more realistic description of the temporal and spatial behavior of the hot and dense matter, the established pictures should be included in the m odel. This makes us approach the comprehensive understanding of the deconned matter, the Quark Gluon Plasma (QGP).

Statistical and hydrodynam ics-m otivated m odels give us the characteristic tem peratures in relativistic heavy-ion collisions. These tem peratures are very useful in understanding what happens in collisions. From thing the model calculation of particle ratios for hadrons to the experimental data, the chemical freeze-out tem perature  $T^{ch}$  is obtained at each collision energy [20, 21, 22, 23, 24, 25]. On the other hand, we can obtain the thermal (kinetic) freeze-out tem perature  $T^{ch}$  from the slopes of transverse momentum distribution by assuming the radial ow prole [22, 26, 27]. The tem peratures obtained above are usually dierent from each other at the AGS, SPS, and probably RHIC energies:  $T^{ch}$  160-200 MeV while  $T^{ch}$  100-140 MeV. The chemical freeze-out parameters ( $T^{ch}$ ;  $T^{ch}$ ) at various collision energies seem to be aligned on one line in the  $T^{ch}$  plane. This line is sometimes called \chemical freeze-out line" and can be parameterized by the average energy per particle  $T^{ch}$  called \chemical freeze-out where the observed particle ratios are xed and next the thermal freeze-out where the

shape of the transverse momentum distribution is xed [28]. Since the time scale of the hydrodynamic evolution is comparable with (or smaller than) that of the inelastic collisions between hadrons, the number changing processes are likely to be out of equilibrium. This is the reason why there are two sequential freeze-out processes in relativistic heavy-ion collisions.

In this paper, we incorporate this picture into hydrodynam ics and discuss how the early chem ical freeze-out a ects the space-time evolution of uids and the particle spectra [29]. In the ordinary hydrodynam ic calculations, one assum esboth chem ical and therm alequilibrium and consequently T ch = T th which is to be determined from comparison of the slopes of transverse spectrum with the experimental data. If the system obeys the above picture of early chem ical freeze-out, those ordinary hydrodynam ic models can hardly reproduce the particle ratios due to the sm allness of the chem ical freeze-out tem perature. As a result, the num ber of resonance particles at the therm al freeze-out becom es too sm all. The physics at the low transverse momentum is largely a ected by resonance decays after thermal freezeout. For example, the low pt enhancement in the transverse momentum spectrum for pions can be explained by the contribution from resonance decays [30, 31]. The slope of the pt spectrum for pions directly emitted from the freeze-out hypersurface is almost constant. On the other hand, data for pions at low pt shows a steeper slope than those in medium pt region ( 1 G eV/c). So one cannot reproduce the low  $p_t$  enhancement only from direct pions. Pions from ,!, or decays show steeperpt spectrum than direct pions. We naturally explain the low pt enhancem ent seen in the experim ental data by resonance decays. A nother exam ple is the reduction of the second Fourier coe cient of the azim uthal distribution for pions at low pt [32]. From the exact treatment of the decay kinematics, pions from resonance decays can pretend out-of-plane elliptic ow even when the hydrodynamic ow shows in-plane elliptic ow. This dilutes elliptic ow from direct pions. Therefore the early chemical freeze-out m ust be included in hydrodynam ics in order to analyze not only the particle ratios but also the single particle spectra and the azim uthal asym metry.

This paper is organized as follows: We construct the equation of state for the hadron phase with and without chemical equilibrium in Sec. II. We parameterize the initial condition for hydrodynamic simulations in the full three dimensional Bjorken coordinate in Sec. III. By using these equations of state and the initial condition, we perform hydrodynamic simulations in full three dimensional space at the RHIC energy and compare space-time evolutions

with each other in Sec. IV. We analyze the particle spectra and the azim uthal asym metry at the RHIC energy and discuss the elect of early chemical freeze-out on observables in Sec. V. We also analyze the two-pion correlation functions to see the elect on the hydrodynamic evolution in Sec. VI. Sum mary and discussions are given in Sec. VII.

# II. EQUATIONS OF STATE

We assume the following picture of space-time evolution for hot and/or dense matter produced in relativistic heavy-ion collisions. First, the huge number of secondary partons are produced and both chemical and thermal equilibrium among these partons are achieved in the early stage of collisions. The initial dominant longitudinal ow and the large pressure gradient perpendicular to the collision axis cause the system to expand and cool down. When the temperature of the system reaches the critical temperature T<sub>c</sub>, the hadronization starts to occur. Just after the hadronization nishes, the chemical freeze-out happens at T d (T<sub>c</sub>). Below T d, the ratios of the number of observed particle are xed. Even after chem ical freeze-out, the system keeps therm alequilibrium through elastic scattering. Finally, all hadrons are thermally frozen at T th (< T ch). If we neglect dissipation in the space-time evolution of nuclear matter, we can apply the hydrodynamic equations for the perfect uid, = 0 and 0  $n_B$  = 0, where T = (E + P)u u Pg and  $n_B$  =  $n_B$ u are energy m om entum tensor and baryon density current, respectively. E, P,  $n_B$ , and u are energy density, pressure, baryon density, and four uid velocity. With the help of therm odynamical identities and the baryon density conservation, the rst equation is rewritten in @ s = 0, where s is the entropy current. These equations mean that a uid element evolves along an adiabatic path ( $n_B = s = const.$ ) in the T -  $_B$  plane. We assume this fact is approximately valid even below chem ical freeze-out line.

When N stable hadrons in the equation of state (EOS) undergo chemical freeze-out across the chemical freeze-out line, we can introduce themical potentials  $_{i}$  associated with those hadrons. Then we may construct the EOS in the (N + 2) dimensional space (N for  $_{i}$  and 2 for T and  $_{B}$ ). This causes a serious problem when we numerically simulate a hydrodynamic model with nite resources of memory. Since the chemical potential of each hadron depends on  $_{B}$ ,  $_{B}$ ,  $_{C}$ , and  $_{B}$ , we can restrict ourselves to the EOS in a two dimensional hypersurface  $_{i} = _{i}$  (T;  $_{B}$ ) embedded in the (N + 2) dimensional space. Thus

we need not prepare such a large dimensional table of the EOS anymore. When we obtain  $_{\rm i}$  at a point (T,  $_{\rm B}$ ) below the chemical freeze-out line, we need the information at the chem ical freeze-out point (T th; th) som ewhere on the chem ical freeze-out line and have to go back to the point along an adiabatic path. Since the adiabatic path itself is obtained from the therm odynam ical variables and  $_{i}(T;_{B})$ , we have to solve the problem self-consistently. In this paper, we restrict our discussion to the zero baryonic chemical potential where the adiabatic path becomes a trivial one,  $n_B = s = 0$ . This is a good approximation in Au + Au p = 130 GeV collisions in which p=p 0:6 [33] or the resultant chem ical freeze-out param eter ch 50 M eV [24].

We construct three models EOS to compare the space-time evolution of uids. These models describe the rst order phase transition between the QGP phase and the hadron phase at  $T_c = 170 \text{ M} \text{ eV}$  . We suppose the QGP phase is composed of massless u, d, s quarks and gluons and that it is comm on to three models. The EOS for the QGP phase is P = (E 4B)=3, where B is a bag constant speci ed later. For the hadron phase, we choose three di erent models EOS as follows.

# A. Chemical Equilibrium

The rst model is an ordinary resonance gas model in which complete chemical equilibrium is always assumed (modelCE). This model is employed for the sake of comparison with the other models. We include strange and non-strange hadrons up to the mass of (1232). Energy density and pressure are as follows:

$$P = \int_{i}^{X} T \frac{d_{i}}{(2)^{3}} d^{3}p \log 1 \exp \frac{q}{p^{2} + m_{i}^{2}} = T; \qquad (2)$$

where  $_{i}$  = 0 due to complete them ical equilibrium in this model. Here the upper and lower signs correspond to bosons and ferm ions. We neglect the excluded volume correction which largely a ects the hadronic EOS in the high baryon density region. From the Gibbs's equilibrium condition at  $T_c = 170 \text{ M}$  eV, we obtain the bag constant B  $^{1=4} = 247.2 \text{ M}$  eV and  $1.7 \,\mathrm{GeV}/\mathrm{fm}^{-3}$ . the latent heat E

#### B. Chem ical Freeze Out

The second model is the simplest one which describes the picture of chemical freeze-out (model CFO). Below  $T^{ch}$ , we assume the numbers of all hadrons  $N_i$  included in the EOS are xed and that the particle number densities obey  $@n_i = 0$ . We introduce a chemical potential  $_i(T)$  associated with each species so that  $N_i$  becomes a conserved quantity. From the conservation of entropy @s = 0, the ratio of the particle number density to the entropy density below the chemical freeze-out temperature obeys

$$\frac{n_{i}(T; _{i})}{s(T; f_{i}g)} = \frac{n_{i}(T_{ch}; _{i} = 0)}{s(T_{ch}; f_{i}g = 0)}$$
(3)

for all hadrons along the adiabatic path. Here we assume  $T^{ch}=170\,\mathrm{M}\,\mathrm{eV}$ , which is consistent with a recent analysis based on a thermal model at the RHIC energy [24]. From Eq. (3), we obtain a chemical potential as a function of temperature for each hadron. The  $_i(T)$  ensures to keep the ratios of the number of each hadron throughout the space-time evolution of a uid element without explicitely solving ( $n_i=0$ ). All chemical potentials are functions of temperature, so the thermodynamical variables depend only on temperature even after them ical freeze-out.

# C. Partial Chemical Equilibrium

The third model represents a more realistic EOS than the second one. The following model is rst discussed in Ref. [34]. The observed particle numbers are always composed of the contribution from direct particles and resonance decays, i.e.,  $N = N + \frac{P}{i6} \tilde{\alpha}_{i!} N_i$ . Here  $\tilde{\alpha}$  is an elective degree of freedom which is a product of the degeneracy d and the branching ratio B. So some processes with large cross sections (e.g., ! ! ) can be equilibrated even below  $T^{ch}$  as long as the equality

$$\frac{n_{i}(T; _{i})}{s(T; f_{i}q)} = \frac{n_{i}(T_{ch}; _{i} = 0)}{s(T_{ch}; f_{i}q = 0)}$$
(4)

is kept instead of Eq. (3). We regard , K , , N , and as \stable" particles 1 and that all them ical potentials can be represented by them ical potentials associated with these stable

Here we use a term \stable" when the lifetime of a hadron is much longer than that of the uid (10 fm/c).

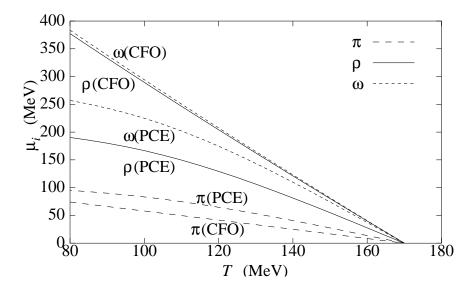


FIG. 1: Chem ical potentials for pions (dashed lines), mesons (solid lines), and ! mesons (dotted lines) for the models CFO and PCE.

particles, e.g., = 2 ,  $_{\rm K}$  = +  $_{\rm K}$ , = +  $_{\rm N}$ , and so on. Thus the third model describes the partial chemical equilibrium (model PCE) even below T <sup>ch</sup> [34].

# D. Chem ical Potentials and Equations of State

Figure 1 shows the chem ical potentials for , , and ! m esons for the m odels CFO and PCE. The di erence of chem ical potentials between hadrons depends only on its mass in the model CFO, so  $_{!}$  (T) behaves like (T) due to the small mass di erence. Both are almost linearly increasing with decreasing temperature. On the other hand, these chem ical potentials di er from each other in the model PCE. It results from each elementary process, i.e., \$ ( = 2 ) and ! \$ ( ! = 3 + 0.88 ), where the branching ratios are from Ref. [35].

One can easily evaluate EOS's for these models by inserting them ical potentials obtained above into Eqs. (1) and (2). We represent pressure and temperature as functions of energy density for three models in Fig. 2. We not in Fig. 2 (a) that pressure as a function of energy density is similar to each other. On the other hand, temperature as a function of energy density in the models CFO or PCE in Fig. 2 (b) is deviated from the model CE. Since the resonance population of the models CFO or PCE is larger than that of the model CE due to the chemical freeze-out, the energy density at a xed temperature in the hadron phase is

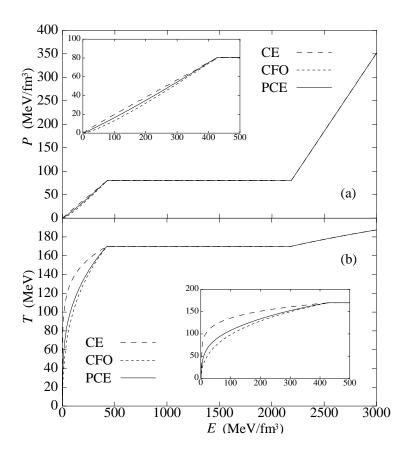


FIG. 2: (a) Pressure as a function of energy density. (b) Temperature as a function of energy density. The dashed, dotted, and solid lines correspond to the models CE, CFO, and PCE.

also large in those models. Conversely, temperature in the models CFO or PCE at a xed energy density is smaller than in the model CE. This fact is very important in qualitatively understanding the dierence of the space-time evolution of uids between three models as shown in Sec. IV.

#### III. IN IT IA L CONDITIONS

We numerically solve the hydrodynam ic equation in the full three dimensional B jorken coordinate ( , s, x, and y) which is relevant to analyze heavy-ion collisions at the collider energies. Here  $=\frac{p}{t^2-z^2}$  and  $_s=(1=2)\log[(t+z)=(t-z)]$  are the proper time and the space-time rapidity, respectively. The x axis is parallel to the impact parameter vector and the y axis is perpendicular to the x axis in the transverse plane. As one of the authors (T H.) has already pointed out [6], the main reason to employ the B jorken coordinate rather than the Cartesian coordinate is a practical one: This considerably reduces numericale orts such

as the long lifetime of uids ( 100 fm/c) and less numerical accuracy near the light cone. In addition to this reason, there is also a physical reason why we avoid to employ the Cartesian coordinate. When one simulates the space-time evolution in the Cartesian coordinate, one gives the initial condition at a constant  $t_0$ . If  $t_0$  is regarded as the thermalization time, this initial condition implies that the thermalization occurs rest from the forward (backward) space-time rapidity in -s coordinate. This is somewhat unrealistic because the multiplicity in the forward rapidity region is much smaller than the one at midrapidity. This may cause a crucial problem when one discusses the rapidity dependence of radial and elliptic ows at the collider energies, since they are sensitive to the thermalization of the system.

We choose initial conditions in the B jorken coordinate so as to reproduce pseudorapidity distribution in Au+Au 130A GeV central (0-6 %) collisions obtained by the PHOBOS Collaboration [36]. At the initial time  $_0 = 0$ :6 fm/c, the initial energy density for central collisions can be factorized as

$$E(x;y;s) = E_{max}W(x;y;b)H(s):$$
 (5)

We assume the transverse prole function W(x;y;b) scales with the impact parameter b in proportion to the number of binary collisions [37]

$$W (x;y;b) / T_{+}T ; T = T (x b=2;y);$$
 (6)

where T (x;y) is a thickness function with the standard W oods-Saxon parameterization for nuclear density

T (x;y) = dz (x;y;z); (x;y;z) = 
$$\frac{p}{\exp[(x^2 + y^2 + z^2) - R_0)} = \frac{1}{1}$$
 (7)

where  $_0=0.17$  fm  $^3$  is the saturation density,  $_0=0.54$  fm is the di useness parameter, and  $R_0=1.12A^{1=3}$   $0.86A^{1=3}$  fm is the nuclear radius. The proportional constant in Eq. (6) is xed from the condition W (0;0;0)=1. The longitudinal probe function H  $(_s)$  is characterized by two parts [6,13,38]: it is at near  $_s$  0 and sm oothly connects to vacuum as a halfpart of the G auss function in the forward and backward space-time rapidity regions

H (<sub>s</sub>) = exp 
$$\frac{(j_s s_0 j_{at}=2)^2}{2 \frac{2}{Gauss}}$$
 (j<sub>s</sub> <sub>s0</sub> j<sub>at</sub>=2): (8)

<sup>&</sup>lt;sup>2</sup> Supposing  $t_0 = 1$  fm/c, the corresponding initial proper time becomes  $t_0 = t_0 = t_0$  0:01 fm/c near the beam rapidity region at RHIC energies.

The length of a at region  $_{at}$  and the width of the Gauss function  $_{Gauss}$  are adjustable parameters to be determined by the experimental data, especially (pseudo) rapidity distribution. In symmetric collisions with the vanishing impact parameter, we expect the symmetry  $E(x;y;_{s}) = E(x;y;_{s})$  holds at the initial time. On the other hand, in non-central (or non-symmetric) collisions, we can shift the energy density by  $_{s0}$  which is identified with the center of rapidity for each transverse coordinate [39]

$$so (x;y;b) = \frac{1}{2} log \frac{(T + T_{+})_{N} + (T - T_{+})_{N} v_{N}}{(T + T_{+})_{N} (T - T_{+})_{N} v_{N}};$$
 (9)

where  $v_N$  and  $v_N$  are, respectively, velocity and Lorentz—factor of an incident nucleon in the center-ofm ass system. For illustrations of the initial energy density, see Ref. [6]. The initial longitudinal ow is the B jorken's solution [40], i.e., the uid rapidity  $v_N = v_N =$ 

Initial parameters in hydrodynamic simulations are so chosen as follows:  $E_{max}=35$  GeV/fm<sup>3</sup>,  $E_{max}=5.8$ ,  $E_{max}=0.2$ , and  $E_{max}=0.2$ ,

# IV. TIME EVOLUTION OF FLUIDS

We simulate the space-time evolution of the uid in the full three dimensional space [6] with the initial conditions and the EOS's discussed in the previous sections. First, we pick up a uid element at the central point  $(x = y = _s = 0)$  and pursue its time evolution till its temperature reaches  $T = 100 \, \text{M}$  eV. Figure 3 shows the time evolution of (a) energy density and (b) temperature at the center of the uid for three models EOS. As far as the time evolution of energy density, we cannot distinguish from each other. This is easily understood by Fig. 2 (a): Energy density evolution is completely governed by the EOS, i.e.,

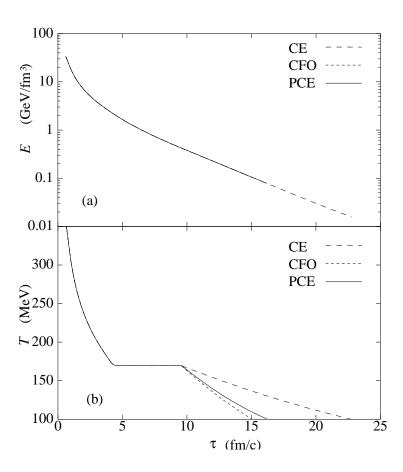


FIG. 3: (a) Time evolution of energy density at the center of the uid. (b) Time evolution of temperature at the center of the uid. The dashed, dotted, and solid lines correspond to the models CE, CFO, and PCE.

P (E) and the three models are very similar to each other. We transform these results from energy density to temperature by using Fig. 2 (b). For the time evolution of temperature, them ical freeze-out makes a substantial dierence between the model CE and the model CFO or PCE. If we suppose them all freeze-out occurs at the constant temperature, the system in which the property of the chemical freeze-out is considered has a fate to be thermally frozen earlier than the conventional model CE. The early chemical freeze-out makes the hadron phase cool down more rapidly [41].

Next, we show how the early chemical freeze-out a ects the spatial size of the uid. Figure 4 represents the time evolution of freeze-out hypersurfaces at  $y = _s = 0$  for (a) the model CE and (b) the model PCE. Here the hypersurfaces in Fig. 4 correspond to various  $T^{th} = 100;120;140$ , and  $160 \, \text{M}$  eV which are within a plausible range for therm all freeze-out temperature. We not that the early chemical freeze-out reduces not only the lifetime of

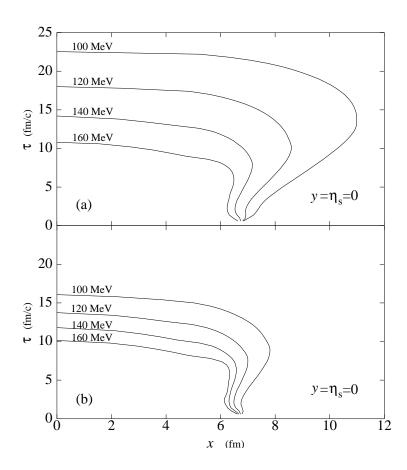


FIG. 4: Space-time evolution of thermal freeze-out hypersurface for (a) the model CE and (b) the model PCE.

the uid but also its spatial size and that the uid does not expand so explosively for the model PCE. Since the two-particle correlation function is sensitive to the spatial size and the lifetime of the uid, it is interesting to see the elect of early chemical freeze-out on the HBT radii. Detailed analyses of pion interferometry will be discussed in Sec.VI.

Figure 5 shows the therm all freeze-out tem perature dependences of average radial ow at m idrapidity <  $v_r > j_{s=0}$ , where  $v_r = \frac{p}{v_x^2 + v_y^2}$ . Radial ow is generated by the pressure gradient, so it contains inform ations about the EOS. From this gure, the radial ow is suppressed when we take account of the early chem ical freeze-out. At T <sup>th</sup> = 140 (120) M eV, the average radial ow for the model PCE is reduced by 17.7 (22.5) % from the one for the conventional model CE.

It should be noted that the di erence between the therm all freeze-out temperature T <sup>th</sup> and the therm all freeze-out energy density E <sup>th</sup> plays an important role in analyses of particle spectra. It m ay be claimed that there are no signicant di erences between three models

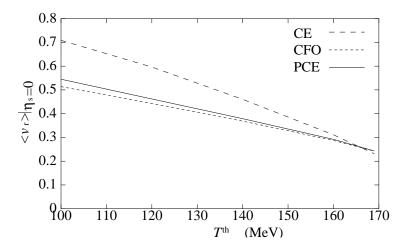


FIG. 5: Therm all freeze-out temperature dependence of average radial ow. The dashed, dotted, and solid lines correspond to the models CE, CFO, and PCE.

when one shows the results in Figs. 4 and 5 as functions of the therm all freeze-out energy density  $E^{th}$ , not temperature  $T^{th}$ . It is indeed true when one discusses only the hydrodynam ic behavior. The shape of particle distribution, especially  $p_t$  spectrum, are determined by the thermal freeze-out temperature  $T^{th}$  and the low in the hydrodynamic model. So this dierence is clearly meaningful when we compare the numerical results of particle spectra with experimental data as shown in the next section.

### V. SINGLE PARTICLE SPECTRA AND AZIM UTHAL ASYM METRY

Hydrodynam ics has a limited prediction power, so the calculation is really meaningful only after tuning the initial parameters and reproducing the single particle spectra. The momentum distribution for particles directly emitted from a (thermal) freeze-out hypersurface can be calculated through the Cooper-Frye formula [42]

$$E \frac{dN}{d^{3}p} = \frac{d}{(2)^{3}} \frac{p}{\exp[(p \ u \ _{i})=T^{th}]} :$$
 (10)

Here, and d are the thermal freeze-out hypersurface and its element. u is the four uid velocity. (+) sign is for boson (ferm ion) and d is the degeneracy of particles under consideration. This formulamerely counts the net particles passing through the hypersurface rather than decoupling from the system. Although it has a problem on the negative number in the treatment of time-like freeze-out hypersurface [43], this is widely used in almost all hydrodynamic models. The observed spectra always contain the contribution

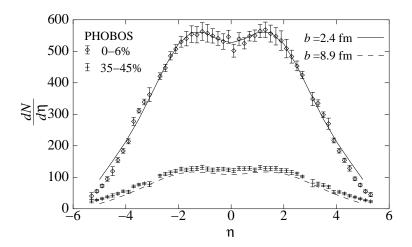


FIG. 6: Pseudorapidity distribution of charged particles in Au+Au 130A GeV collisions. Data from Ref. [36].

from resonance decays. We assume all of the resonance particles in the EOS are also emitted from a freeze-out hypersurface and that they decay into stable particles. Taking account of the decay kinematics, we easily obtain the single particle spectra from resonance particles [31, 32]. For further details to calculate the spectra from resonance decays, see Appendix.

Figure 6 shows the pseudorapidity distribution of charged particles in Au + Au 130A GeV collisions. The num erical results correspond to the model PCE with T<sup>th</sup> = 140 MeV. From the analyses based on the wounded nucleon model, we choose the impact parameter b = 2.4 fm for 0-6% central collisions and b = 8.9 fm for 35-45% non-central collisions. The resultant number of participants is 342 (94) for b = 2.4 (8.9) fm, which is consistent with estimation by the PHOBOS Collaboration [36]. We reasonably reproduce the data in not only central but also non-central collisions by using initial parameters in the previous section. A fiter tuning initial parameters for central events, we have no adjustable parameters for non-central events due to assuming the binary collision scaling. For non-central collisions, we change the impact parameter in Eq. (6) as to the number of participants with keeping other parameters in the initial condition. A Ithough the binary collisions contribute to hard components, the binary collision scaling seems to be reasonable to parameterize the hydrodynamic initial condition [37] from Fig. 6.

We next show in Fig. 7 the pt spectrum for negative charged hadrons. The experimental

<sup>&</sup>lt;sup>3</sup> When we calculate the two-pion correlation function in the next section, we neglect this contribution for simplicity.

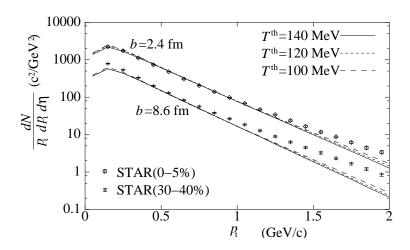


FIG. 7: Transverse m om entum spectra of negative charged particles in Au + Au 130A G eV collisions. The dashed, dotted, and solid lines correspond to  $T^{th} = 100$ , 120, and 140 M eV. D at a from Refs. [44] and [45].

data (0-5% central [44] and 30-40 % semicentral events [45]) are observed by the STAR Collaboration. The impact parameters used in this calculation are b = 2.4 fm for central and b = 8:6 fm for sem icentral events. We represent the therm alfreeze-out temperature dependence of pt spectrum for the model PCE. The slope of pt spectrum is almost independent 1 GeV/c, which is a little peculiar behavior in the usual sense. However, it is interpreted by the result in Fig. 5. When one reduces the thermal freeze-out temperature by hand, the average radial ow enhances as its response. The magnitude of the response is governed by the EOS. The resultant pt slope is a competition between these two e ects: The reduction of tem perature makes the slope steeper in the case of vanishing ow, while the therm ald istribution is Lorentz-boosted by radial ow and the  $p_t$  slope becomes atter. The e ect of generated radial ow on the pt slope usually overcomes that of the reduction of T  $^{\rm th}$  in the model CE, so the  $p_{\rm t}$  slope becomes atter as decreasing T  $^{\rm th}$ . On the other hand, the radial ow is slightly suppressed in the model PCE as shown in Fig. 5. Hence the reduction of T th is just compensated by its response to radial ow for the model PCE. This is the reason why the  $p_t$  slope is almost independent of T th in Fig. 7. In any T th within a plausible range, we reproduce the experimental data below 1 GeV/c for central collisions. This indicates that there exists the onset of hard processes around  $p_t$  1 GeV/c. For sem i central collisions, we also reproduce the slope of the  $p_t$  spectrum below 1 GeV/c. It should be noted that a bend of the spectrum in low pt region is simply due to the Jacobian between

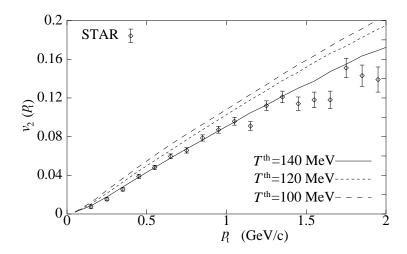


FIG. 8:  $v_2$  ( $p_t$ ) for charged hadrons in Au+Au 130A GeV collisions. The dashed, dotted, and solid lines correspond to T <sup>th</sup> = 100, 120, and 140 M eV .D ata from Ref. [46].

the pseudorapidity and the rapidity Y.

We next show the transverse momentum dependence of the second Fourier coecient for azim uthal distribution for the model PCE. Figure 8 represents  $v_2$  ( $p_t$ ) for charged particles in minimum bias collisions. Experimental data is also observed by STAR [46]. Hydrodynamic analysis of the data has already been done by Kolbet al. [47]. They found the hydrodynamic result excellently coincides with the data below  $p_t$  1:5 GeV/c. Now we not the space-time evolution in our model is dierent from their result where them ical equilibrium is always assumed, we must check whether the hydrodynamic description is really good at RHIC even when we include the elects of early them ical freeze-out. The numerical results are calculated from the following equation:

$$v_{2}(p_{t}) = \frac{P R}{b} \frac{d d \cos(2) b_{p_{t}dp_{t}d d} (p_{t}; ; b)}{P R} = \frac{dN}{b} \frac{dN}{d b_{p_{t}dp_{t}d} (p_{t}; ; b)} (11)$$

Here the sum mation with respect to the impact parameter b is taken over every 2 fm up to 14 fm in this analysis. The integral region of is from 1:3 to 1:3, which corresponds to the analysis by STAR [46]. The value of  $v_2$  ( $p_t$ ) depends on the thermal freeze-out temperature  $T^{th}$  in contrast with the  $p_t$  spectrum. We also reproduce the experimental data below 1 GeV/c by choosing  $T^{th}=140$  MeV and slightly overestimate the data above 1 GeV/c. Similar to the  $p_t$  spectrum, this result also indicates that the hard contribution, which reduces  $v_2$  calculated from hydrodynamic source [5,48], becomes important above 1 GeV/c.

Figure 9 separately represents the contribution of pions directly emitted from freeze-out

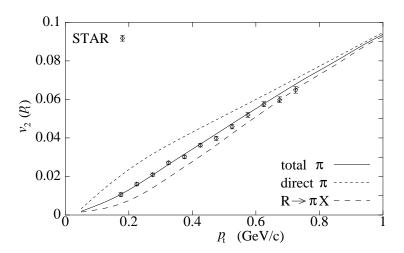


FIG. 9:  $v_2$  ( $p_t$ ) for charged pions. The solid, dotted, and dashed lines correspond to total pions, pions directly emitted from freeze-out hypersurface, and pions from resonance decays. Data from Ref. [49].

hypersurface and the contribution of pions from resonance decays. The STAR data shows the contribution from identi ed pions [49]. From this gure, the concavity of  $v_2$  ( $p_t$ ) in low  $p_t$  region ( $p_t < 0.3\,\text{G\,eV}/\text{c}$ ) results from the resonance decay after them all freeze-out. The exact treatm ent of the decay kinem atics of resonances dilutes  $v_2$  for direct pions especially in low  $p_t$  region [32]. The fraction of the contribution from resonance decays plays a very important role in understanding  $v_2$  ( $p_t$ ) for pions in low  $p_t$  region, so the early chemical freeze-out must be included when we discuss proper phenomena to the low transverse momentum.

In Fig. 10, we compare the pseudorapidity dependence of elliptic ow between the models CE and PCE. Similar to the  $v_2$  ( $p_t$ ),  $v_2$  () which is to be compared with minimum bias data is

$$v_{2}() = \frac{P R}{b P_{t}dp_{t}d \cos(2) b \frac{dN}{p_{t}dp_{t}d d} (p_{t}; ; b)} = \frac{P R}{b P_{t}dp_{t}} \frac{R}{b P_{t}dp_{t}d d} (p_{t}; ; b)}$$
(12)

We choose  $T^{th}=140\,\text{M}$  eV and integrate with respect to  $p_t$  from 0 to 2.0 GeV/c. Data plots are observed by PHOBOS [50]. The rectangular area corresponds to the statement by STAR [46],  $v_2()=4:5$  0:5% for 0:1 <  $p_t$  < 2:0 GeV/c and j ; 1:3. As well as the case of radial ow, the elliptic ow is also reduced by taking account of the chemical freezeout. We reproduce the PHOBOS data only near mid (pseudo) rapidity and overestimate in forward and backward rapidity. On the other hand, a microscopic transport model (JAM) reproduces the data only in forward and backward rapidity regions [51]. This indicates

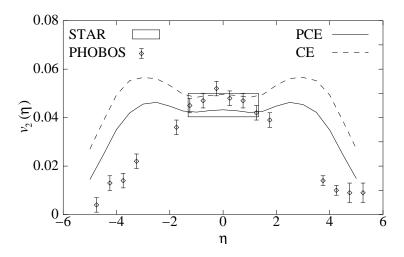


FIG. 10:  $v_2$  () for charged hadrons in Au+Au 130A GeV collisions. The solid and dashed lines correspond to the models PCE and CE.D ata from Refs. [46] and [50].

that the full therm alization is achieved only nearm idrapidity, although there are some open problems in hydrodynamics such as the treatment of freeze-out through the Cooper-Frye formula, more sophisticated initialization, and the absorption by spectators [6].

From Figs. 8 and 10, the hydrodynam ic description with early chemical freeze-out seems to be valid for, at least,  $0 < p_t < 1 \, \text{GeV/c}$  and  $1 < < 1 \, \text{in Au+Au}$  collisions at 130A GeV.

# VI. PION INTERFEROMETRY

From the single particle spectra and the azim uthal asym metry, we obtain the information about the distribution in the momentum space at freeze-out. On the other hand, we can obtain the information about the particle distribution in the coordinate space through two-particle interferometry [52]. We see in Sec. IV the space-time evolutions are considerably dierent between the models with and without chemical equilibrium. To see this more clearly, we discuss the two-pion correlation function in this section.

In hydrodynam ics, the two-particle correlation function for directly em itted bosons from

freeze-out hypersurface can be calculated from [53, 54]

$$C_{2}(p_{1};p_{2}) = \frac{P(p_{1};p_{2})}{P(p_{1})P(p_{2})}$$

$$= 1 + \frac{\frac{\frac{d}{(2)^{3}}R}{K} d \exp(ix q) f(\frac{Ku}{T^{th}})^{2}}{E_{1}\frac{dN}{d^{3}p_{1}}E_{2}\frac{dN}{d^{3}p_{2}}};$$
(13)

Here P  $(p_1;p_2)$  is the two particle coincidence cross section and P  $(p_1)$  is the same Cooper-Frye form ula represented in Eq. (10). We consider only directly emitted pions for simplicity.  $K = (p_1 + p_2) = 2$  and  $q = p_1$   $p_2$  are, respectively, the average and relative four momentum of pair.  $f_{BE} = (e^x - 1)^{-1}$  is the Bose-Einstein distribution function. The informations about hydrodynamic simulations enter through the freeze-out hypersurface and the four velocity u in this equation. The average pair momentum K is decomposed into the transverse momentum  $K_T$ , the longitudinal momentum  $K_Z$ , and the azimuthal angle  $K_Z$ . The relative pair momentum  $K_Z$  is also decomposed into the standard coordinate,  $K_Z$  (parallel to  $K_T$ ),  $K_Z$  (along the beam direction), and  $K_Z$  (perpendicular to the others). Since the experimental acceptances are limited to midrapidity, jy  $K_Z$  0.5 (STAR) [55] or  $K_Z$  0.35 (PHENIX) [56], we can put  $K_Z$  = 0. Moreover, we average the two-particle function  $K_Z$  over the azimuthal angle  $K_Z$ . Thus we obtain the following equation which can be compared with the experimental data:

$$C_{2}(K_{T};q_{side};q_{but};q_{long}) = \frac{R}{R} \frac{R}{R} \frac{P(p_{1};p_{2})}{(p_{1})P(p_{2})}$$
(14)

Our de nition of the HBT radii is similar to the one in Refs. [54, 57, 58]. Assuming that  $C_2$  (K  $_{\rm T}$ ;  $q_{\rm side}$ ;  $q_{\rm but}$ ;  $q_{\rm long}$ ) for each K  $_{\rm T}$  is tted by the Gaussian form

$$C_2 = 1 + \exp(R_{\text{side}}^2 q_{\text{side}}^2 - R_{\text{out}}^2 q_{\text{out}}^2 - R_{\text{long}}^2 q_{\text{long}}^2)$$
 (15)

with a chaoticity = 1, the K  $_{\text{T}}$  dependence of HBT radius for the side direction is  $R_{\text{side}}(K_{\text{T}}) = 1 = q_{\text{side}}(K_{\text{T}})$ , where  $C_{2}(K_{\text{T}};q_{\text{side}};0;0) = 1 + e^{-1}$ , and analogous de nitions for the K  $_{\text{T}}$  dependence of  $R_{\text{out}}$  and  $R_{\text{long}}$ .

We evaluate two-pion correlation functions for negative pions directly em itted from freeze-out hypersurface and obtain the K  $_{\rm T}$  dependence of R  $_{\rm side}$ , R  $_{\rm out}$ , and R  $_{\rm long}$ . Figure 11 shows

 $<sup>^4</sup>$  Even for central events, we have no longer cylindrical sym m etry around the collision axis due to small (but nite) value of the impact parameter, so C  $_2$  depends on the azim uthal angle  $_{\rm K}$  which is measured from the reaction plane.

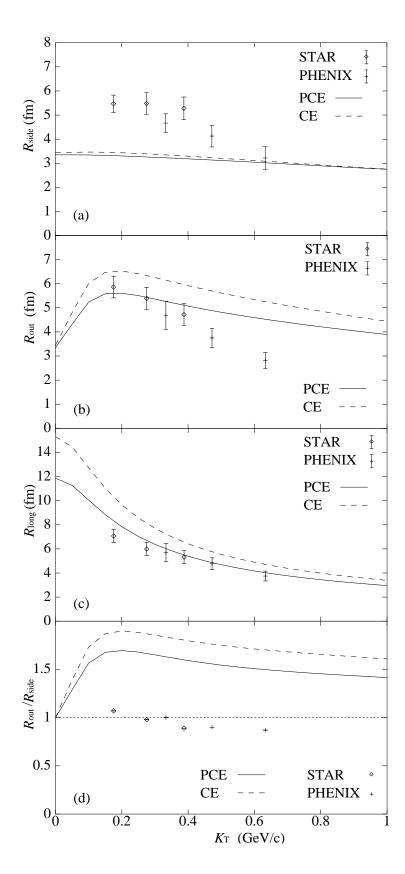


FIG.11: HBT radii for negative pions in (a) side, (b) out, and (c) long direction and (d) its ratio  $R_{\text{out}}=R_{\text{side}}$  as a function of  $K_{\text{T}}$ . The solid and dashed lines correspond to the models PCE and CE.D ata from Refs. [55] and [56].

the HBT radii and the ratio  $R_{out}=R_{side}$  for the models CE and PCE with  $T^{th}=140~M~eV$ . Here the impact parameter which we choose in this analysis is b=2.4~fm. The dierence between the two models is very small for  $R_{side}$ . On the other hand,  $R_{out}$  and  $R_{long}$  for the model PCE are significantly smaller than the ones for the model CE, which rejects the space-time evolution of freeze-out hypersurface depicted in Fig. 4. We compare our results with experimental data observed by STAR (12% most central events) [55] and PHENIX (30% most central events) [56]. We reproduce the  $K_T$  dependence of  $R_{long}$  by employing the model PCE, while  $R_{side}$  and  $R_{out}$  do not show good coincidences with the experimental data.

It has been suggested that the ratio R  $_{\rm out}$ =R  $_{\rm side}$  re ects the prolongation of the lifetime due to the phase transition between the QGP phase and the hadron phase [54]. Various m odels predict this ratio has a value signi cantly larger than unity in some K  $_{\rm T}$  region [38, 54, 57, 58, 59], although it is around unity in  $0.2 < {\rm K}_{\rm T} < 0.6 {\rm GeV/c}$  in Au + Au  $^{\rm P}$   $_{\rm S_{N\,N}}$  = 130A GeV collisions according to the recent m easurement at RHIC [55, 56]. This discrepancy is often called \the HBT puzzle" [59, 60]. The ratio for the model PCE reduces by about 12% above  $0.2 {\rm GeV/c}$  due to the property of the early chemical freeze-out, but it clearly turns out to be larger than the experimental data. Our aim in this paper is to see how the early chemical freeze-out a ects the HBT radii, so we leave detailed discussions on the HBT puzzle in the future works.

# VII. SUM MARY AND DISCUSSION

We have investigated the elect of early chemical freeze-out on the hydrodynamic evolution and the particle spectra by using a genuine three dimensional hydrodynamic model. We constructed the equation of state for hadronic matter which is in partial chemical equilibrium. Pressure as a function of energy density is not a ected by the chemical non-equilibrium property, while temperature as a function of energy density is largely reduced due to the large population of resonance particles. By using the EOS with a rest order phase transition, we simulated hydrodynamic evolution at the RHIC energy. We found the system cools down more rapidly than the conventional model and that the lifetime and the spatial size of the uid and the radial and elliptic lows are reduced when we compared at isothermal hypersurface. We also analyzed particle spectra and two-pion correlation functions in Au+Au

130A GeV collisions. We chose initial parameters in the hydrodynamic simulations so as to reproduce the pseudorapidity distribution in central collisions observed by PHOBOS. The slope of pt spectrum for negative hadrons is less sensitive to the therm al freeze-out tem perature, which results from the reduction of radial ow. On the other hand, the transverse m om entum dependence of elliptic ow  $v_2$  (p<sub>t</sub>) for charged hadrons depends on the therm al freeze-out tem perature. The situation is completely opposite to the ordinary hydrodynam ic results. In the conventional models, the  $p_t$  slope is steeper as increasing T<sup>th</sup> and  $v_2$  ( $p_t$ ) is not so sensitive to Tth. We found Tth = 140 MeV and the resultant average radial ow <  $v_{\rm r}>$  = 0.38c are the values to simultaneously reproduce the  $p_{\rm t}$  slope and  $v_{\rm 2}$  ( $p_{\rm t}$ ) below  $1 \text{ GeV} \cdot v_2$  ( ) is also reduced by the early chemical freeze-out, but we failed to reproduce the data in forward and backward rapidity regions. In order to see more quantitatively the e ect of early chemical freeze-out on the temporal or spatial size of uids, we calculated the two-pion correlation functions and obtained the HBT radii. By taking account of the early chem ical freeze-out in the EOS,  $R_{out}$ ,  $R_{long}$ , and  $R_{out}$ = $R_{side}$  are signi cantly suppressed, while R side is not changed. Nevertheless, the properties of the early chemical freeze-out are not enough to interpret the HBT puzzle.

These studies suggest that attention should be paid to the early chem ical freeze-out in hydrodynam ics. Some results from conventional hydrodynam ics in the literature should be revisited by incorporating the properties of chem ical freeze-out. Penetrating probes such as therm alphotons and dileptons may also be a ected by the early chem ical freeze-out. The emission rates of photons or dileptons increase due to the chemical potentials for hadrons, while the space-time volume of the hadron phase decreases. Therefore we should check whether the total multiplicity and spectra of photons and dileptons are changed in terms of hydrodynamics.

There are other approaches to describe the early chem ical freeze-out. The model evolves the QGP and mixed phases as a relativistic uid, while it switches to a hadronic cascade model, e.g., UrQMD [61] or RQMD [62]. The advantage over these hybrid models is to be able to obtain the average hydrodynam ic behavior and the elect of temperature naturally. When one discusses the spectral changes of hadrons due to the medium elects such as temperature and/or baryonic chemical potential [63], one can easily estimate its elect by using hydrodynamic simulations. We regard the model PCE as a complementary tool to those hybrid models.

A free publishing our prelim inary results [29] and almost nishing this work, the authors are aware of a paper concerning the same subject [64], in which the conclusion on the hydrodynam ic behavior is almost the same as ours. In Ref. [64], the e ect of nite baryonic chemical potential is included but the hydrodynam ic simulation is performed only in the transverse plane by assuming the B jorken's scaling solution.

# A cknow ledgm ents

The authors thank m em bers in high-energy physics group at W aseda University for useful comments and K.Kajim oto for his collaboration in the early stage of this work. One of the author (T.H.) acknowledges valuable discussion with T.Hatsuda, P.Huovinen, K.Morita, S.Muroya, H.Nakamura, C.Nonaka, D.Rischke. He also thanks Inoue Foundation for Science for nancial support.

\*

# APPENDIX A: MONTE CARLO CALCULATION OF THE CONTRIBUTION FROM RESONANCE DECAYS

In this appendix, we show how to calculate the particle distribution from resonance decays within the Cooper-Frye prescription. This method can be used in hydrodynamics-motivated models as well as in hydrodynamics.

Lorentz transform ation for the momentum of a decay particle between the local rest system (starred) and the nite momentum system (non-starred) of a resonance particle R is

$$p = p p_R \frac{E}{m_R} \frac{p_R}{m_R (m_R + E_R)}$$
 : (A1)

We rewrite Eq. (A1) explicitly

w here

$$F(p_1; ) = \frac{E(p_1; )}{m_R} \frac{p_t(p_1; )p_{Rt}\cos( _R) + p_1p_{R1}}{m_R(m_R + E_R)};$$
 (A4)

Here the independent variables which we choose for decay particles are the longitudinal momentum  $p_1$  and the azimuthalangle . Thus the transverse momentum of a decay particle  $p_t$  is written in terms of  $p_1$  and

$$p_{t}(p_{1}; ) = \frac{1}{q^{R} \frac{[1 \quad v_{Rt}^{2} \cos^{2}( \quad _{R})]}{(E + p_{1}v_{R1R})^{2} \quad (p_{1}^{2} + m^{2})^{\frac{2}{R}} [1 \quad v_{Rt}^{2} \cos^{2}( \quad _{R})]} : (A 5)$$

The Jacobian of the Lorentz transform ation is de ned by

$$dp_1d = J(p_1; ;V_R)dp_1d;$$
 (A 6)

$$J(p_1; ; V_R) = \begin{pmatrix} \frac{e_{p_1}}{e_{p_1}} & \frac{e_{p_1}}{e} \\ \frac{e}{e_{p_1}} & \frac{e}{e} \end{pmatrix} : \qquad (A7)$$

The calculation of J is straightforward, so that we do not represent it here. The normalization of momentum space volume for a decay particle in the resonance rest frame is

$$\frac{Z_p}{\int_{p}^{p} \frac{dp_1}{2p} \int_{0}^{\frac{q}{2}} \frac{d}{2} = 1$$
: (A8)

We always average the decay probability over the spin of resonances, so that the decay probability does not depend on  $p_1$  and  $p_2$ . Thus the normalization in the resonance reference frame is

$$\frac{J(p_1; ; V_R)dp_1d}{4p} = 1:$$
 (A 9)

The Jacobian in Eq. (A 7) has very narrow peaks when the resonance particle moves at a large velocity in the laboratory system [32]. This singularity makes it dicult to integrate the Jacobian numerically. So we introduce a very simple Monte Carlo calculation to evaluate the momentum distribution from resonance decays. All input parameters in this calculation are the numerical results of hydrodynamic simulation, i.e., the temperature  $T^{th}$ , the chemical potential for resonance particles  $_R$ , the three-dimensional unid velocity v, and the element don the freeze-out hypersurface. In the following discussion, we show how to obtain the rapidity distribution of negative pions, for simplicity, only from mesons. In this case, the branching ratio  $B_{0(1)} = 0$ . It is straightforward to extend this scheme to the cases for other resonances or the transverse mass (momentum) distribution.

Step 1: Evaluate the number of  $\,^0$  and  $\,^0$  which are emitted from or absorbed by the k-th freeze-out hypersurface element d  $_k$ :

N<sub>k</sub><sup>R</sup> = 
$$\frac{g_R}{(2)^3} = \frac{d^3p_R}{E_R} = \frac{jp_R}{\exp[(p_R)_{k} - p_R) = T^{th}]} = 1$$
: (A 10)

The integrand does not contain the Jacobian, so that it is simple to carry out the numerical integration by a standard technique. It should be noted that  $N_k^R$  is dierent from the net number of emitted mesons from the k-th uid element and that this is used merely for normalization.

Step 2: Generate N random momenta  $P_j$  (1 j N) for mesons which obey the distribution

$$\frac{P^{2}}{q - \frac{1}{P^{2} + m_{P}^{2}}} = T^{th} = 1$$
(A 11)

Here we om it the Breit-Wigner function for simplicity.

Step 3: For each N random momentum  $P_j$ , generate random variables (  $_j$ ;  $_j$ ) whose ensemble is uniformly distributed on the unit sphere. By using these random variables, we obtain an ensemble of meson with momentum  $P_j = (P_{xj}; P_{yj}; P_{zj}) = (P_j \sin_j \cos_j; P_j \sin_j \sin_j p_j \cos_j)$ , which obeys the Bose-Einstein distribution in the uid rest system .

Step 4:Boost P  $_{\mbox{\scriptsize j}}$  with respect to the  $% \left( 1\right) =\left( 1\right) +\left( 1\right)$ 

$$P_{j} = P_{j} + v_{k} \quad E_{j} + \frac{P_{j} \quad v_{k}}{1 + v_{k}}$$
; (A 12)

where  $_k = 1 = p \frac{p}{1 - v_k^2}$ .

Step 5: Generate N´ uniform random variables on the unit sphere (j; j) and obtain an ensemble of negative pions with momentum  $p_j = (p_{xj}; p_{yj}; p_{zj}) = (p \sin j \cos j; p \sin j \sin j; p \cos j)$ , where p is given by

$$p = \frac{1}{2m_R} q \frac{q}{(m_R + m_R)^2 m_X^2} (m_R m_R)^2 m_X^2$$
 (A 13)

For the decay process ! ,  $m_X = m$ .

Step 6:Boost  $p_i$  with respect to the resonance momentum  $P_j$ 

$$p_{j} = p_{j} + P_{j} \frac{E_{j}}{m_{p}} + \frac{p_{j} P_{j}}{m_{p} (m_{p} + E_{p})}$$
 (A 14)

Step 7: If  $P_i$  d k is positive,

$$N_{k}^{+} ! N_{k}^{+} + \frac{P_{j} d_{k}}{E_{j}}$$
 (A 15)

If P d k is negative,

$$N_{k} ! N_{k} + \frac{jP_{j}d_{k}j}{E_{j}}$$
: (A16)

Here,  $N_k^+$  ( $N_k$ ) is to be proportional to the number of mesons which are emitted from (absorbed by) the k-th uid element.

Step 8: If the rapidity of a negative pion  $Y_j$  which is evaluated from  $p_j$  enters in a rapidity window  $Y = \frac{Y}{2} < Y_j < Y + \frac{Y}{2}$  and  $P_j$  d k is positive,

$$N_{k}^{+}(Y)! N_{k}^{+}(Y) + \frac{P_{j}d_{k}}{E_{j}}:$$
 (A 17)

If  $Y_j$  also enters the above rapidity window but  $P_j$  d  $_k$  is negative,

$$N_{k}(Y)! N_{k}(Y) + \frac{jP_{j}d_{k}j}{E_{j}}$$
 (A18)

Step 9: Repeat steps 7 and 8 for all N random variables.

Step 10:0 btain the rapidity distribution of decay particles from the k-th uid element

$$\frac{dN_{k}}{dY}(Y) = \frac{N_{k}^{R}}{N_{k}^{+} + N_{k}} - \frac{N_{k}^{+}(Y) - N_{k}(Y)}{Y} :$$
 (A 19)

It should be noted that the m inus sign in the bracket of Eq. (A 19) means the net number of em itted particles from the k-th uid element, which is consistent with the Cooper-Frye prescription. For the normalization in Eq. (A 19), we use the gross number  $N_k^+ + N_k^-$  since this number is positive denite.

Step 11: Repeat the above steps from 1 to 10 for all uid elements obtained in a numerical simulation of the hydrodynamic model. Summing over the contribution from all uid elements on the freeze-out hypersurface, we obtain the rapidity distribution of negative pions which are from decays:

$$\frac{dN_{!} \times X}{dY} (Y) = \frac{X}{dY} \frac{dN_{k}}{dY} (Y):$$
 (A 20)

<sup>[1]</sup> S.A.Bass, Nucl. Phys. A 698, 164 (2002); X.N.W ang, ibid. A 698, 296 (2002).

<sup>[2]</sup> P. Huovinen, nucl-th/0204029.

<sup>[3]</sup> K.Adcox et al. (PHENIX), Phys. Rev. Lett. 88, 022301 (2002).

- [4] R.J.M. Snellings (STAR), Nucl. Phys. A 698, 193 (2002).
- [5] M.Gyulassy, I.Vitev, X.N.W ang, and P.Huovinen, Phys. Lett. B 526, 301 (2002).
- [6] T.Hirano, Phys. Rev. C 65, 011901 (2002).
- [7] J.-Y.Ollitrault, Phys. Rev. D 46, 229 (1992).
- [8] D. Teaney and E. V. Shuryak, Phys. Rev. Lett. 83, 4951 (1999).
- [9] P.F.Kolb, J. Sollfrank, and U. Heinz, Phys. Rev. C 62, 054909 (2000).
- [10] U.Omik, M.Plumer, B.R.Schlei, D.Strottman, and R.M.Weiner, Phys.Rev.C 54, 1381 (1996).
- [11] J. Sollfrank, P. Huovinen, M. Kataja, P. V. Ruuskanen, M. Prakash, and R. Venugopalan Phys. Rev. C 55, 392 (1997).
- [12] C.M. Hung and E.V. Shuryak, Phys. Rev. C 57, 1891 (1998).
- [13] K.Morita, S.Muroya, H.Nakamura, and C.Nonaka, Phys.Rev.C 61, 034904 (2000); T.Ishii and S.Muroya, Phys.Rev.D 46, 5156 (1992).
- [14] N.S.Amelin, E.F. Staubo, L.P. Csemai, V.D. Toneev, K.K. Gudima, and D. Strottman, Phys. Rev. Lett. 67, 1523 (1991).
- [15] D. H. Rischke, S. Bernard, and J. A. Maruhn, Nucl. Phys. A 595, 346 (1995); D. H. Rischke, Y. Pursun, and J. A. Maruhn, ibid. A 595, 383 (1995).
- [16] C.Nonaka, E.Honda, and S.Muroya, Eur. Phys. J.C 17, 663 (2000).
- [17] T.Hirano, K.Tsuda, and K.Kajim oto, nucl-th/0011087.
- [18] T.O sada, C.E.A guiar, Y.Hama, and T.Kodama, nuclth/0102011.
- [19] V.K.Magas, L.P.Csemai, and D.Strottman, hep-ph/0202085.
- [20] J.C. Leym ans and H. Satz, Z. Phys. C 57, 135 (1993).
- [21] P.Braun-Munzinger, J.Stachel, J.P.W essels, and N.Xu, Phys.Lett.B 344, 43 (1995); 365, 1 (1996); P.Braun-Munzinger, I.Heppe, and J.Stachel, ibid. 465, 15 (1999).
- [22] J. Cleymans and K. Redlich, Phys. Rev. Lett. 81, 5284 (1998); Phys. Rev. C 60, 054908 (1999).
- [23] F.Becattini, J.Cleymans, A.Keranen, E.Suhonen, and K.Redlich, Phys.Rev.C 64,024901 (2001).
- [24] P.Braun-Munzinger, D.Magestro, K.Redlich, and J.Stachel, Phys. Lett. B 518, 41 (2001).
- [25] M.Kaneta and N.Xu, J. Phys. G 27, 589 (2001).
- [26] E. Schnederm ann, J. Sollfrank, and U. Heinz, Phys. Rev. C 48, 2462 (1993).

- [27] W. Broniowski and W. Florkowski, Phys. Rev. Lett. 87, 272302 (2001).
- [28] See, for exam ple, E.V. Shuryak, Nucl. Phys. A 661, 119 (1999); U. Heinz, Nucl. Phys. A 661, 140 (1999).
- [29] For our prelim inary results, see, T. Hirano and K. Tsuda, nucl-th/0202033.
- [30] U.Omik and R.M.Weiner, Phys. Lett. B 263, 503 (1991).
- [31] J. Sollfrank, P. Koch, and U. Heinz, Z. Phys. C 52, 593 (1991).
- [32] T. Hirano, Phys. Rev. Lett. 86, 2754 (2001).
- [33] C.Adler et al. (STAR), Phys. Rev. Lett. 86, 4778 (2001); B.B.Back et al. (PHOBOS), Phys. Rev. Lett. 87, 102301 (2001); I.G.Bearden et al. (BRAHMS), Phys. Rev. Lett. 87, 112305 (2001); K.Adcox et al. (PHENIX), nuclex/0112006.
- [34] H. Bebie, P. Gerber, J. L. Goity, and H. Leutwyler, Nucl. Phys. B 378, 95 (1992).
- [35] D.E.Groom et al. (Particle Data Group Collaboration), Eur. Phys. J. C 15, 1 (2000).
- [36] B.B.Back et al. (PHOBOS), Phys. Rev. Lett. 87, 102303 (2001).
- [37] P.F.Kolb, U.Heinz, P.Huovinen, K.J.Eskola, and K.Tuom inen, Nucl. Phys. A 696, 197 (2001).
- [38] T. Hirano, K. Morita, S. Muroya, and C. Nonaka, nuclth/0110009 (to be published in Phys.Rev.C).
- [39] J. Sollfrank, P. Huovinen, and P. V. Ruuskanen, Eur. Phys. J. C 6, 525 (1999).
- [40] J.D.B prken, Phys. Rev. D 27, 140 (1983).
- [41] N. Arbex, F. Grassi, Y. Hama, and O. Socolowski, Phys. Rev. C 64, 064906 (2001).
- [42] F.Cooper and G.Frye, Phys.Rev.D 10, 186 (1974).
- [43] Y. M. Sinyukov, Z. Phys. C 43, 401 (1989); K. A. Bugaev, Nucl. Phys. A 606, 559 (1996);
  C. Anderlik, Z. I. Lazar, V. K. Magas, L. P. Cæmai, H. Stocker, and W. Greiner, Phys. Rev.
  C 59, 388 (1999); C. Anderlik, L. P. Cæmai, F. Grassi, W. Greiner, Y. Hama, T. Kodama,
  Z. I. Lazar, V. K. Magas, and H. Stocker, ibid. 59, 3309 (1999).
- [44] C.Adler et al. (STAR), Phys. Rev. Lett. 87, 112303 (2001).
- [45] M. Calderon de la Barca Sanchez, nucl-ex/0111004.
- [46] K.H.Ackerm ann et al. (STAR), Phys. Rev. Lett. 86, 402 (2001).
- [47] P.F.Kolb, P.Huovinen, U.Heinz and H.Heiselberg, Phys.Lett. B 500, 232 (2001).
- [48] X.-N.W ang, Phys.Rev.C 63, 054902 (2001); M.G yulassy, I.V itev, and X.N.W ang, Phys. Rev.Lett.86, 2537 (2001).

- [49] C.Adler et al. (STAR), Phys. Rev. Lett. 87, 182301 (2001).
- [50] I.C.Park et al. (PHOBOS), Nucl. Phys. A 698, 564 (2002).
- [51] P.K. Sahu, in the proceedings of the International Conference on Physics and Astrophysics of Quark-Gluon Plasma (ICPAQGP-2001), Kolkata, 2001 (to be published).
- [52] See, for example, G. Baym, Acta Phys. Pol. B 29, 1839 (1998); U. Heinz and B. V. Jacak, Ann. Rev. Nucl. Part. Sci. 49, 529 (1999).
- [53] B.R. Schlei, U.Omik, M. Plumer, and R.M. Weiner, Phys. Lett. B 293, 275 (1992).
- [54] D.H.Rischke and M.Gyulassy, Nucl. Phys. A 608, 479 (1996).
- [55] C.Adler et al. (STAR), Phys. Rev. Lett. 87, 082301 (2001).
- [56] K.Adcox et al. (PHENIX), nuclex/0201008.
- [57] S.So, S.A.Bass, and A.Dum itru, Phys. Rev. Lett. 86, 3981 (2001).
- [58] D. Zschiesche, S. Schramm, H. Stocker, and W. Greiner, nucl-th/0107037.
- [59] U. Heinz and P. F. Kolb, Nucl. Phys. A 702, 269 (2002); hep-ph/0204061.
- [60] S.So, hep-ph/0202240.
- [61] S.Bass and A.Dum itnu, Phys. Rev. C 61, 064909 (2000).
- [62] D. Teaney, J. Lauret, and E. V. Shuryak, Phys. Rev. Lett. 86, 4783 (2001); nucl-th/0110037.
- [63] See, for exam ple, T. Hatsuda, Nucl. Phys. A 698, 243 (2002).
- [64] D. Teaney, nucl-th/0204023.